Available online at www.sciencedirect.com
ScienceDirect
Progress in Natural Science 18 (2008) 913–919
Progress in Natural Science
www.elsevier.com/locate/pnsc

Review

# An overview on SAR measurements of sea surface wind

Hui Lin [a], Qing Xu [a,*], Quanan Zheng [b]

[a] Institute of Space and Earth Information Science, The Chinese University of Hong Kong, Room 615, Esther Lee Building, Hong Kong, China
[b] Department of Atmospheric and Oceanic Science, University of Maryland, College Park, MD, USA

Received 27 November 2007; received in revised form 24 March 2008; accepted 24 March 2008

**Abstract**

Studies show that synthetic aperture radar (SAR) has the capability of providing high-resolution (sub-kilometer) sea surface wind fields. This is very useful for applications where knowledge of the sea surface wind at fine scales is crucial. This paper aims to review the latest work on sea surface wind field retrieval using SAR images. As shown, many different approaches have been developed for retrieving wind speed and wind direction. However, much more work will be required to fully exploit the SAR data for improving the retrieval accuracy of high-resolution winds and for producing wind products in an operational sense.


*Keywords:* SAR; Sea surface wind; Wind retrieval algorithms

## 1. Introduction

Sea surface wind is a crucial parameter for the studies of sea surface variables such as waves, ocean circulation, marine meteorology and the coupling of oceanic and atmospheric systems. These variables can be measured from space by both active and passive microwave instruments such as scatterometers (SCATs), altimeters, SARs and radiometers. Among these instruments, satellite SCATs can measure global winds with a spatial resolution of up to 25 km on an operational basis. The SCAT winds, with the accuracy of wind speed and direction of $\pm 2\ \mathrm{m\ s^{-1}}$ and $\pm 20°$, respectively, have been assimilated into forecast models for a variety of weather and climate studies. However, the relatively low spatial resolution makes the SCAT winds best suited for the open ocean studies. Thus the observation of short-scale wind features from SCATs is not possible. In contrast, satellite SARs with all-weather capability and large spatial coverage, have a higher spatial resolution and therefore have the potential to provide wind fields over the sea surface with spatial resolution nearly two orders higher (sub-kilometer) than conventional SCATs. This will enhance the understanding of marine atmospheric boundary layer and oceanographic processes, especially in coastal areas.

For incidence angles between 15° and 70° [1], the radar backscatter from the sea surface is primarily caused by the small-scale sea surface roughness, which is strongly influenced by the local wind field. This creates the possibility of extracting sea surface wind from SAR images. Early investigations of extracting the wind field from SAR images were made in Refs. [2] and [3], which demonstrated a correlation between the L-band SEASAT SAR image intensity and SEASAT scatterometer wind speed. Then Ref. [4] described the linear features aligned with the direction of the wind on the scale of a few kilometers in SEASAT images. Using Fourier transform techniques, the wind direction, albeit with a 180° ambiguity, was estimated from the wind row caused linear features. Following SEASAT, several satellites carrying SARs which work at different bands and polarizations have been launched. Based on the large amount of SAR data, different wind retrieval methods were then developed.

* Corresponding author. Tel.: +852 31634082; fax: +852 26037470.
*E-mail address:* Xuqing215@yahoo.com.cn (Q. Xu).

1002-0071/$ - see front matter 
doi:10.1016/j.pnsc.2008.03.008

In this paper, we will give a brief overview of the latest study on wind field retrieval from SAR images. The methods for estimating only of wind speed and wind direction are introduced in Sections **2 and 3**, respectively. In Section **4** methods for simultaneous retrieval of wind speed and wind direction from SAR images are presented. Section **5** is conclusions.

## 2. Wind speed retrieval

Among the approaches for wind speed retrieval the most widely used ones are based on the methods of retrieving sea surface wind speed from SCATs. These methods are introduced in the first part. Some other alternative approaches for solely wind speed retrieval are presented in the second part of this section.

### 2.1. Scatterometry-based approaches

In scatterometry-based approaches, the dependency of the normalized radar cross-section (NRCS) of radar sensors (e.g., SCATs or SARs) on the wind speed and the geometry of observations (e.g., incidence angle and azimuth angle with respect to wind direction) is generally expressed by the geophysical model function (GMF). We summarize the general form of the function as

$$\sigma_0 = A(U_{10},\theta)[1 + b_1(U_{10},\theta)\cos\phi + b_2(U_{10},\theta) \times \cos 2\phi]^B \quad (1)$$

where $\sigma_0$ is the NRCS in linear units; $\phi$ is the relative wind direction, which represents the angle between the radar look direction and the local wind direction; $U_{10}$ is the statistically neutral wind speed normalized to 10 m height; $\theta$ is the incidence angle and $A$, $B$, $b_1$ and $b_2$ are coefficients depending on $U_{10}$, $\theta$, radar frequency and polarization.

Fig. 1 shows a general flow for wind retrieval from a SAR image using scatterometry-based approaches. With wind directions from either the SAR image itself or from outside sources (e.g., *in situ* data, SCAT measurements, or atmospheric model outputs) and a GMF, the wind speeds can be derived from the SAR image.

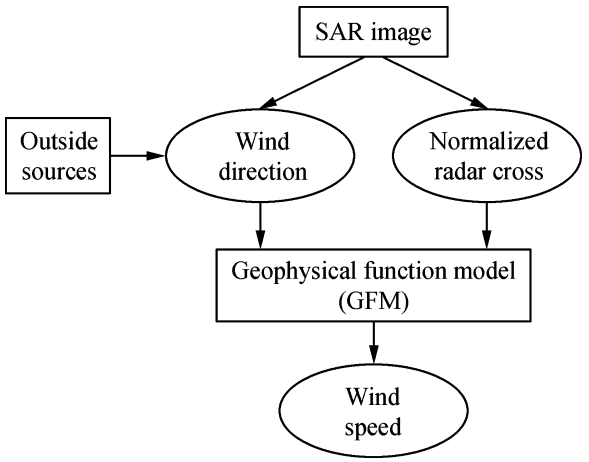


Fig. 1. Schematic description of wind retrieval from SAR images using scatterometry approaches.

#### 2.1.1. Wind speed retrieval from VV-polarized SAR

For the instruments operating at C-band and vertical (VV) polarization in transmission and reception, several empirical GMFs have been developed and validated through a series of satellite scatterometer missions. The most widely used are CMOD4 [5] developed and empirically tuned to ECMWF (the European Center for Medium-Range Weather Forecast) weather model results, CMOD_IFR2 [6] developed at Ifremer-France and calibrated against *in situ* measurements, in particular NOAA buoys and partly ECMWF model results, and CMOD5 [7] which was an upgrade of CMOD4 to address certain wind speed biases in the CMOD4 model function. It has been shown that these functions are applicable for wind speed retrieval from VV-polarized SARs onboard ERS-1 and ERS-2 and ENVISAT [8–14]. Fig. 2 shows the SAR-estimated NRCS as a function of sea surface wind speed. The NRCSs are computed by CMOD4, CMOD_IFR2 and CMOD5, respectively. Although CMOD5 is more suitable for estimating high wind speeds stronger than 25 m $s^{-1}$ [7]. Fig. 2 shows that all CMOD functions produce very similar results for wind speeds below 20 m $s^{-1}$. For different regions where GMF is the most appropriate, it is still an open question.

For L-band and VV-polarized SAR, a model function has been developed [15]. The L-band model enables wind

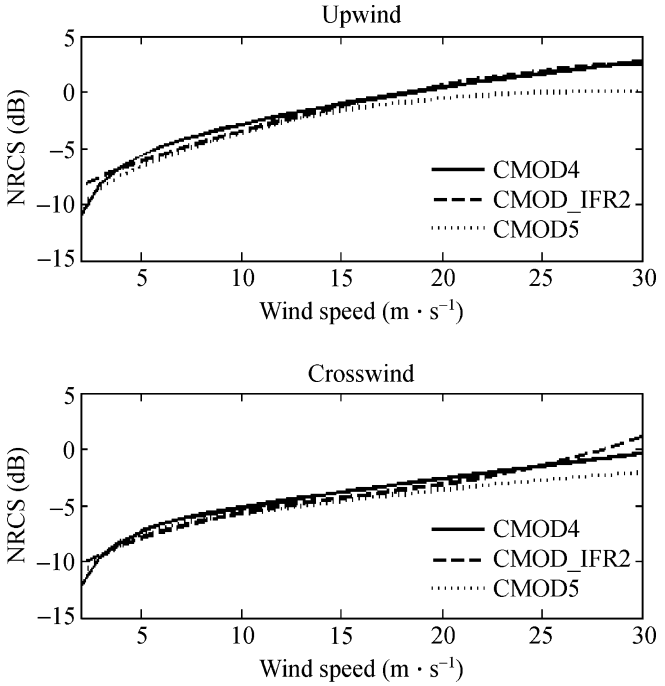


Fig. 2. NRCS as a function of the wind speed computed by various C-band model functions as indicated in the figure. The incidence angle is 25°, and the relative wind directions are 0° (upwind, upper panel) and 90° (crosswind, lower panel), respectively.

speed retrieval from SAR onboard JERS-1 (Japanese Earth Resources Satellite-1).

*2.1.2. Wind speed retrieval from HH-polarized SAR*

For wind speed retrieval from SAR images acquired at horizontal (HH) polarization in transmission and reception (e.g., SAR onboard RADARSAT-1), no well developed models exist, but two approaches have been attempted. The first and more widely used approach has been to develop a hybrid model function consisting one of the VV-polarized GMFs and a polarization ratio [16–22]. The second has been to derive analytical models directly for HH polarization [23].

In the first approach, the polarization ratio Pr is defined as

$$\mathrm{Pr} = \frac{\sigma_0^{\mathrm{VV}}}{\sigma_0^{\mathrm{HH}}} \tag{2}$$

where $\sigma_0^{\mathrm{VV}}$ and $\sigma_0^{\mathrm{HH}}$ are the NRCS values in VV and HH polarizations, respectively.

The polarization ratio has been measured by Unal et al. [24] with an airborne SCAT for incidence angles of 20°, 30° and 45° for wind speeds at 2–14 m $s^{-1}$. Their study showed that the ratio is mainly dependent on the incidence angle. But for wind speeds below 6 m $s^{-1}$, a wind speed dependency was also observed. By fitting a model to the data of Ref. [24], Thompson et al. proposed a polarization ratio model relating Pr to the incidence angle in the following form [25]:

$$\mathrm{Pr} = \frac{(1 + 2\tan^2\theta)^2}{(1 + \alpha\tan^2\theta)^2} \tag{3}$$

where Pr is in linear units; $\alpha$ is a constant relating to the type of surface scattering and was set to 0.6. This relation keeps a general form consistent with both the Bragg condition ($\alpha = 0$) and the geometrical optics (or Kirchhoff) condition ($\alpha = 2$). Ref. [26] compared RADARSAT SAR wind speeds derived by the CMOD2_IFR2 model with buoy measurements and determined that $\alpha \approx 1$, which was also suggested by Horstmann et al. [16]. From five dual-polarization (HH and VV) ENVISAT ASAR images, Ref. [27] expressed the polarization ratio as a polynomial function of $\tan(\theta)$ for incidence angles below 30° and made the ratio follow the form of Eq. (3) with $\alpha = 1$ at incidence angles higher than 30°.

Another form of the polarization ratio is [28]

$$\mathrm{Pr} = \frac{(1 + 2\tan^2\theta)^2}{(1 + 2\sin^2\theta)^2} \tag{4}$$

which yields NRCS values in HH polarization in better agreement with the SASS-2 model derived from the Ku-band SASS (Seasat-A Satellite Scatterometer) measurements than the classical one.

Based on the data from C-band airborne radar STORM, Ref. [29] proposed two analytical formulations to model the polarization ratio, one as an exponential function of the incidence angle only and the second one with additional dependency on the azimuth angle. The models have been assessed by ENVISAT ASAR images.

Fig. 3 shows the polarization ratio of (3) with $\alpha$ of 0.6 and 1, the form from Ref. [27], and the ratio of (4), together with the exponential form from Ref. [29]. The figure shows that the polarization ratios differ from each other with exception for those in Refs. [25] and [27] at incidence angles higher than 30°. The difference between various polarization ratios may be due to the sensitivity of the polarization ratio to the calibration uncertainty of different radars.

*2.2. Alternative approaches*

Besides the scatterometry-based approaches, several emerging methods for wind speed retrieval have also been developed in the recent years.

*2.2.1. Azimuth cut-off method*

The fundamental idea behind this method is the extraction of the wind speed from the sea surface wave spectrum. Based on the evaluation of 1200 SAR wave mode images with a central incidence angle of 20.2°, in the case of a fully developed sea (no fetch limitation), an empirical relation between $U_{10}$ and the azimuth cut-off wave length $\lambda_c$ was given in Ref. [30] as

$$U_{10} = 4.75\left(\frac{\lambda_c - 30}{110}\right) \tag{5}$$

The cut-off wave length can be estimated in the spectral domain either by fitting the auto covariance function (ACF) derived from an inverse Fourier transform of the SAR image power spectrum with a Gaussian function [31] or by fitting the ACF with more sophisticated models [32].

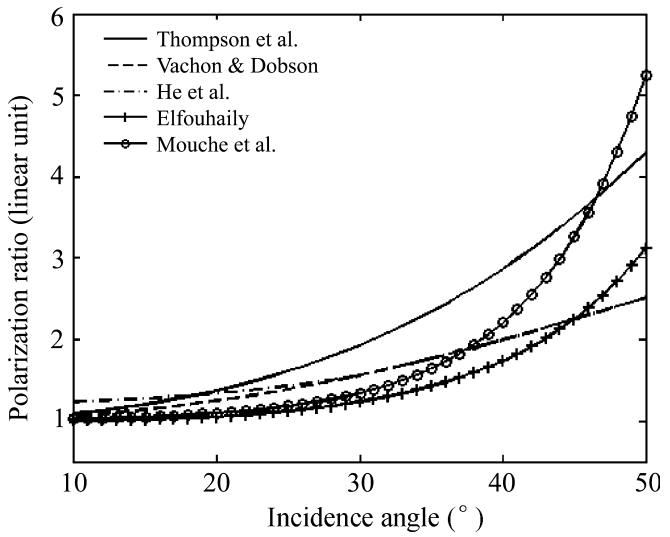


Fig. 3. Polarization ratio as a function of the incidence angle from various formulations as indicated in the figure.

The main advantage of this approach is that no information on wind direction is required. However, the approach only holds for C-band, VV polarization and low incidence angles (~20°). When using this approach, one must also be cautious since the cut-off wave length estimate includes long wave orbital motion contributions which may contaminate the result.

*2.2.2. Neural network method*

For uncalibrated SAR images, the neural network (NN) method allows the retrieval of wind speed directly from the SAR image intensity, independent of any knowledge of the NRCS. The method does not require explicit models for the SAR imaging process and can therefore be applied to any system configuration, i.e., polarization, incidence angle, etc. [33]. Ref. [33] applied this method to wind retrieval from SLC ERS-2 SAR wave mode images on a global and continuous basis, and the derived wind speeds agreed well with ERS-2 SCAT measurements. The NN method may also be applicable for retrieving both wind speed and wind direction from calibrated images. However, no results from such investigations have been reported.

*2.2.3. Physical model*

Studies show that the contribution of specular reflection to the NRCS received by the radar is also significant at incidence angles less than 30° [34]. Considering the contribution of both specular reflection and Bragg scattering to NRCS, a physical model [35] was applied to wind speed retrieval from SAR images. The physical wind model can retrieve wind speeds from either VV- or HH-polarized SAR images. The comparison of wind speeds measured by five buoys in Hong Kong coastal waters to those retrieved from 30 VV-polarized ENVISAT ASAR images from October 2005 to June 2007 using the CMOD4, CMOD_IFR2, CMOD5 and the physical model, respectively, shows that the physical model is comparable with the C-band empirical models (see Fig. 4a–d where *RMSE*, *Bias* and *R* denote root mean square error, bias and correlation coefficient, respectively).

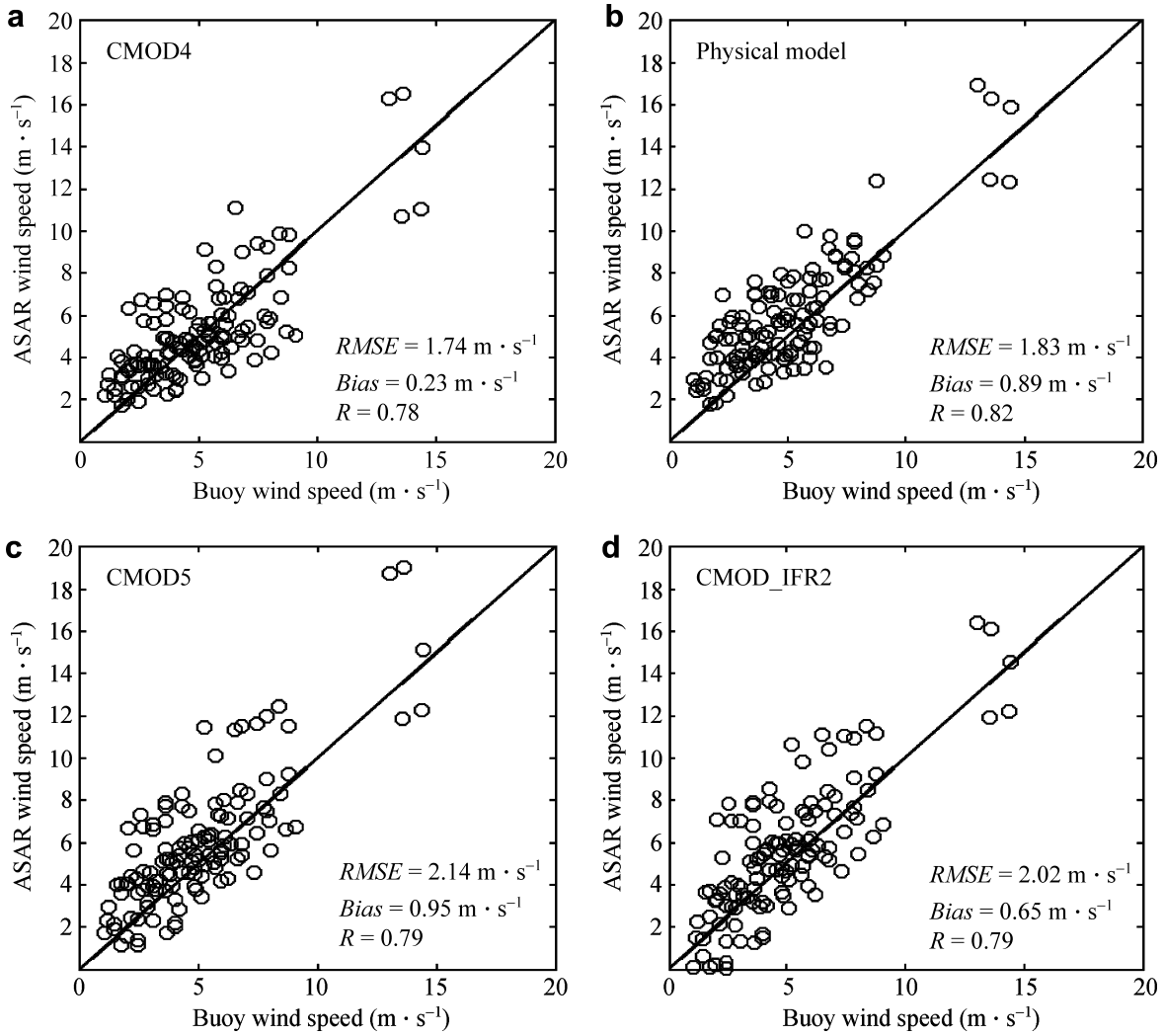


Fig. 4. Comparison of buoy measurements with wind speeds retrieved from VV-polarized ENVISAT ASAR images using CMOD4 (a), physical model (b), CMOD5 (c) and CMOD_IFR2 (d), respectively.

## 3. Wind direction retrieval

To measure wind speeds from SAR images using wind direction dependent methods such as the scatterometry-based approaches, the main difficulty is the lack of knowledge of the wind direction. To solve this problem, there are different methods in use, for example, assuming a fixed direction from a measurement for the whole image, or interpolation of the wind direction from SCATs or atmospheric models. Despite the empirical success of SAR wind speed retrieval using such wind direction, the above approaches ignore wind direction information in the SAR image itself. In SAR images, if the linear features aligned with the wind direction are visible, the wind direction can be derived directly from the images. These features, however, could be caused by any of the several physical effects, e.g., marine atmospheric boundary layer rolls [4,36], Langmuir cells, surfactant streaks, or wind shadowing [8,37,38].

Several methods have been developed to retrieve the orientation of the linear features aligned with the wind direction in SAR images. These methods can be divided into two categories: one is in the spectral domain, the other in the spatial domain.

In the spectral domain, the most popular method is the Fast Fourier Transform (FFT) method, which was first described by Gerling [4] and then modified and applied by several others [8,10,16,17,26,31,37,39–41]. In this method, the Fourier spectrum of the SAR image is computed. The main spectral energy is located perpendicular to the orientation of the wind streaks, giving a wind direction with a 180° directional ambiguity. The 180° directional ambiguity is a very important issue and is hard to remove. It can be removed only if wind shadowing is present which is often visible in the lee of coastlines, or if there are additional data available, e.g., wind direction from *in situ* data, SCAT measurements, or atmospheric model outputs. With a relatively low-resolution of wind direction retrieval such as $20 \times 20$ km$^2$, the FFT method works fine on open oceans.

A significant problem with the FFT method is that there may not be a feature aligned with the wind in all the parts of the image. Thus the method will often generate erroneous directions over featureless regions of the image. To address this problem, Ref. [42] developed a projection method based on projections of the image values at various angles, which can automatically estimate wind direction only from the image locations containing sufficient linear features. For the regions with no appropriate features, wind directions can be interpolated from the surrounding directions.

In the spatial domain, a recently developed wind direction retrieval method is the local gradient (LG) method, which derives the orientation of the wind streak by computing the local gradient on different scales [12,18,43]. Alternative approaches such as wavelet analysis [44,45] and variance method [46] have also been applied. Compared with the spectral analysis, the spatial analysis improves the resolution of SAR direction retrieval to better than $10 \times 10$ km$^2$ and even to $1 \times 1$ km$^2$ [43].

Although wind direction can be derived from the linear features on SAR image itself, it should be noted that not all SAR images contain linear features aligned with the wind direction. Moreover, the presence of long wind waves and other atmospheric features visible in some images are difficult to separate from these linear features. To solve these problems, emerging methods have been developed for retrieving wind direction from SAR images. These methods, to be introduced in Section **4**, are capable of estimating wind speed simultaneously and have been called wind vector retrieval methods.

## 4. Wind vector retrieval

### 4.1. Optimal inversion method

Based on a general statistical approach to solve inversion problems (including underdetermined problems) in meteorological analysis, Ref. [47] proposed a SAR wind retrieval method which can estimate wind speed and direction simultaneously. This simplified method combines the SAR information, i.e., NRCS and/or wind induced streaks, with some background information coming from high-resolution limited area model or buoy data to retrieve the most probable wind speed and wind direction, assuming that all sources of information contain errors and that these are well characterized. The comparison of the wind vectors retrieved from this method and that from the scatterometry approach indicated that the optimal inversion method showed a promising result. However, *a priori* information (background wind data) would be required for this approach.

### 4.2. Multiple NRCS method

This method was recently developed by He et al. [48] and was applied to ASAR images. It was motivated by the methodology used for SCAT data, in which the wind vectors are determined from multiple NRCSs measured by SCATs with different look directions. In this method, a given SAR image was divided into many blocks along the radar look direction and the radar flight direction, respectively. Wind vectors can be retrieved by using multiple NRCSs from two neighboring blocks along the radar look direction, which have slightly different incidence angles. A constraint on this method is that the wind speeds retrieved from ASAR images in the near range tend to be underestimated, which may be due to the underestimation of NRCS related to the saturation effect of the SAR analog-to-digital conversion (ADC) in the near range.

### 4.3. Dual-polarization method

The method for retrieving the wind vector using dual-polarization ASAR images was developed by Song et al. [49]. Based on the combination of two ASAR images with co-polarization and cross-polarization, the wind vector can be retrieved by solving three equations with only two

Table 1
Summary of approaches for sea surface wind retrieval

| Wind speed | Wind direction | Advantages | Disadvantages |
|---|---|---|---|
| Scatterometry-based approaches | / | Validated by large amounts of data. In quasi-operational use | One-dimensional wind component. Wind direction dependent |
| Azimuth cut-off method | / | Independent of wind direction and image calibration | One-dimensional wind component. Limited to low incidence angle. Fetch dependent |
| Neural network method | / | Independent of image calibration. Available for any system configuration (radar frequency, incidence angle, polarization, etc.) | One-dimensional wind component |
| Physical model | / | Available for any polarization | One-dimensional wind component. Wind direction dependent |
| / | Model output | Always available. Reasonable directions | Low-resolution. Space/time mismatch with SAR images |
| / | Alternative data (*in situ*, SCAT, etc.) | Independently validated directions | Low-resolution. Space/time mismatch |
| / | From linear features in SAR image (FFT, LG, etc.) | Space/time exact match. Higher-resolution than model output or alternative data | Not always available. Contaminated by other features and 180° ambiguity of wind direction |
| Optimal inversion method | | Using both SAR data and background model data | Requires *a priori* information and a set of assumptions |
| Multiple NRCS method | | Independent of *a priori* information | Underestimation of wind speed in the near range. 180° ambiguity of wind direction |
| Dual-polarization method | | Independent of *a priori* information Eliminates 180° ambiguity of wind direction | Requires SAR with both co-polarization and cross-polarization |

unknown variables, e.g., wind speed and wind direction. In this way, the 180° directional ambiguity occurring when a single SAR image is used can be effectively eliminated. But this method is only applicable for wind retrieval from SAR with both co-polarization and cross-polarization, such as ASAR.

## 5. Conclusions

SARs can measure sea surface wind fields with high-resolution at sub-kilometer scales. As mentioned above, different approaches have been developed to estimate wind parameters (wind speed and/or wind direction) from SAR images. Each approach has its advantages and drawbacks. Table 1 is a summary of these approaches. Among the different approaches, the scatterometry-based approaches for wind speed retrieval and FFT or LG methods for wind direction retrieval are the ones mostly used and have been applied to the quasi-operational environment [19]. Comparisons with buoy measurements in the previous studies show an accuracy of better than 1.8 m $s^{-1}$ for wind speed in the 2–20 m $s^{-1}$ wind speed range and better than 20° for wind direction [20,38,48] with a 180° ambiguity. Comparisons with SCAT measurements show a random error of wind speed and wind direction even better than 1.0 m $s^{-1}$ and 15°, respectively [21,33,49,50].

Although various wind retrieval approaches have been suggested, the sea surface wind retrieval from SAR images is still in its infancy, since it was developed only 10 years ago. Much more work is required to understand how we can fully exploit the SAR data for improving the retrieval accuracy of high-resolution winds. As data sets, including SAR images, sea surface winds and wind data from other sources, e.g., SCATs and atmospheric model outputs continue to grow, SAR wind retrieval performance can be statistically evaluated, high-resolution SAR winds can be provided in an operational sense, and the full evaluation of SAR winds can be realized.

## Acknowledgements

This work was supported by ITC (Grant No.GHP/026/06), RGC (Grant No. 461907), and partly by ONR (Grant No. N00014-05-1-0328 and N00014-05-1-0606 for Zheng).

## References

[1] Holt B. SAR imaging of the ocean surface. In: Synthetic aperture radar marine user's manual. Washington, DC: US Government Printing Office; 2004. 464, p. 25–80.
[2] Jones WL, Delnore VE, Bracalente EM. The study of mesoscale ocean winds. In: Spaceborne synthetic aperture radar for oceanography. Baltimore: Johns Hopkins University Press; 1981, p. 87–94.
[3] Weissman DE, King D, Thompson TW. Relationship between hurricanes surface winds and L-band radar backscatter from the sea surface. J Appl Meteor 1979;18:1023–34.
[4] Gerling TW. Structure of the surface wind field from the Seasat SAR. J Geophys Res 1986;91:2308–20.
[5] Stoffelen A, Anderson D. Scatterometer data interpretation: estimation and validation of the transfer function CMOD4. J Geophys Res 1997;102:5767–80.

[6] Quilfen Y, Chapron B, Elfouhaily T, et al. Observation of tropical cyclones by high-resolution scatterometry. J Geophys Res 1998;103:7767–86.
[7] Hersbach H. CMOD5: an improved geophysical model function for ERS C-band scatterometry. European Centre for Medium Range Weather Forecasting (ECMWF) Technical Memorandum 2003;395:1–50.
[8] Fetterer F, Gineris D, Wackerman CC. Validating a scatterometer wind algorithm for ERS-1 SAR. IEEE Trans Geosci Remote Sens 1998;36:479–92.
[9] Furevik BR, Korsbakken E. Comparison of derived wind speed from synthetic aperture radar and scatterometer during the ERS tandem phase. IEEE Trans Geosci Remote Sens 2000;38:1113–21.
[10] Lehner S, Horstmann J, Koch W, et al. Mesoscale wind measurements using recalibrated ERS SAR images. J Geophys Res 1998;103:7847–56.
[11] Horstmann J, Koch W, Lehner S. Ocean wind fields retrieved from the advanced synthetic aperture radar aboard ENVISAT. Ocean Dyn 2004;54:570–6.
[12] Horstmann J, Koch W. Measurement of sea surface winds using synthetic aperture radars. IEEE Trans Geosci Remote Sens 2005;30:508–15.
[13] Horstmann J, Thompson DR, Monaldo F, et al. Can synthetic aperture radars be used to estimate hurricane force winds? Geophys Res Lett 2005;32:L22801, doi: 10.1029/2005GL023992.
[14] Shimada T, Kawamura H. Statistical compartmentalization of surface wind field over coastal seas using high-resolution SAR-derived winds. Geophys Res Lett 2005:32, doi:10.1029/2004GL022231.
[15] Shimada T, Kawamura H, Shimada M. An L-band geophysical model function for SAR wind retrieval using JERS-1 SAR. IEEE Trans Geosci Remote Sens 2003;41:518–31.
[16] Horstmann J, Koch W, Lehner S, et al. Wind retrieval over the ocean using synthetic aperture radar with C-band HH polarization. IEEE Trans Geosci Remote Sens 2000;38:2122–31.
[17] Horstmann J, Lehner S, Koch W, et al. Computation of wind vectors over the ocean using spaceborne synthetic aperture radar. John Hopkins Univ Tech Digest 2000;21:100–7.
[18] Horstmann J, Koch W, Lehner S, et al. Ocean winds from RADARSAT-1 ScanSAR. Can J Remote Sens 2002;28:524–33.
[19] Monaldo FM. The Alaska SAR demonstration and near real-time synthetic aperture radar winds. Johns Hopkins Univ Tech Digest 2000;21:75–84.
[20] Monaldo FM, Thompson DR, Beal RC, et al. Comparison of SAR-derived wind speed with model predictions and ocean buoy measurements. IEEE Trans Geosci Remote Sens 2001;39:2587–600.
[21] Monaldo FM, Thompson DR, Pichel WG, et al. A systematic comparison of QuikSCAT and SAR sea surface wind speeds. IEEE Trans Geosci Remote Sens 2004;42:283–91.
[22] Thompson DR, Beal RC. Mapping high resolution wind fields using synthetic aperture radar. Johns Hopkins Univ Tech Digest 2000;21:58–67.
[23] Wackerman CC, Clemente-Colón P, Pichel W, et al. A two-scale model to predict C-band VV and HH normalized radar cross section values over the ocean. Can J Remote Sens 2002;28:367–84.
[24] Unal CMH, Snooji P, Swart PJF. The polarization-dependent relation between radar backscatter from the sea surface and surface wind vectors at frequencies between 1 and 18 GHz. IEEE Trans Geosci Remote Sens 1991;29:621–6.
[25] Thompson DR, Elfouhaily TM, Chapron B. Polarization ratio for microwave backscattering from the ocean surface at low to moderate incidence angles. In: Geoscience and Remote Sensing Symposium Proceedings, IGARSS '98;1998;3:1671–3.
[26] Vachon PW, Dobson FW. Wind retrieval from RADARSAT SAR Images: selection of a suitable C-band HH polarization wind retrieval model. Can J Remote Sens 2000;26:306–13.
[27] He Y, Zou Q, Perrie W. Validation of wind vector retrieval from ENVISAT ASAR images. In: Geoscience and Remote Sensing Symposium, IGARSS '04; 2004;5:3184–7.
[28] Elfouhaily TM. Modèle couple vent/vagues et son application à la télédétection par micro-onde de la surface de la mer, Ph.D. thesis, Univ Paris VII, Paris, France; 1996 [in French].
[29] Mouche AA, Hauser D, Daloze JF, et al. Dual-polarization measurements at C-band over the ocean: results from airborne radar observations and comparison with ENVISAT ASAR data. IEEE Trans Geosci Remote Sens 2005;43:753–69.
[30] Chapron B, Fouhaily TE, Kerbaol V. Calibration and validation of ERS wave mode products. IFREMER document DRO/OS/95-02, Brest, France; 1995.
[31] Lehner S, Schulz-Stellenfleth J, Schattler B, et al. Wind and wave measurements using complex ERS-2 SAR wave mode data. IEEE Trans Geosci Remote Sens 2000;38:2246–57.
[32] Hasselmann S, Brüning C, Hasselmann K, et al. An improved algorithm for the retrieval of ocean wave spectra from synthetic aperture radar image spectra. J Geophys Res 1996;101:16615–29.
[33] Horstmann J, Schiller J, Schulz-Stellenfleth J, et al. Global wind speed retrieval from SAR. IEEE Trans Geosci Remote Sens 2003;41:2277–86.
[34] Liu Y, Yan XH, Liu WT, et al. The probability density function of ocean surface slopes and its effects on radar backscatter. J Phys Oceanogr 1997;27:782–97.
[35] Xu Q, Lin H. Ocean surface wind retrieval from ENVISAT ASAR images in Hong Kong adjacent waters. In: Proceedings of the First International Conference on Environmental Remote Sensing for Pearl River Delta Region. Hong Kong, China, 10–11 January; 2008.
[36] Alpers W, Brümmer B. Atmospheric boundary layer rolls observed by the synthetic aperture radar aboard the ERS-1 satellite. J Geophys Res 1994;99(6):12613–22.
[37] Vachon PW, Dobson FW. Validation of wind vector retrieval from ERS-1 SAR images over the ocean. Global Atmos Ocean Syst 1996;5:177–87.
[38] Dankert H, Horstmann J, Rosenthal W. Ocean winds fields retrieved from radar-image sequences. J Geophys Res 2003;108:3352.
[39] Wackerman CC, Rufenach R, Johannessen J, et al. Wind vector retrieval using ERS-1 synthetic aperture radar imagery. IEEE Trans Geosci Remote Sens 1996;34:1343–52.
[40] Kerbaol K, Chapron B. Analysis of ERS-1/2 synthetic aperture radar wave mode imagettes. J Geophys Res 1998;103:7833–46.
[41] Korsbakken E, Johannessen JA, Johannessen OM. Coastal wind retrievals from ERS synthetic aperture radar. J Geophys Res 1998;103:7857–74.
[42] Wackerman CC, Pichel W, Li X, et al. Estimation of surface winds from SAR using a projection algorithm. In: Proceedings of the 14th Conference on Satellite Meteorology and Oceanography; 2006, J4.4.
[43] Koch W. Directional analysis of SAR images aiming at wind direction. IEEE Trans Geosci Remote Sens 2004;42:702–10.
[44] Du Y, Vachon PW, Wolf J. Wind direction estimation from SAR images of the ocean using wavelet analysis. Can J Remote Sens 2002;28:498–509.
[45] Fichaux N, Rachin T. Combined extraction of high spatial resolution wind speed and direction from SAR images: a new approach using wavelet transform. Can J Remote Sens 2002;28:510–6.
[46] Wackerman CC, Horstmann J, Koch W. Operational estimation of coastal wind vectors from RADARSAT SAR imagery. In: Geoscience and Remote Sensing Symposium, IGARSS '03; 2003;2:1270–2.
[47] Portabella M, Stoffelen A, Johannessen JA. Toward an optimal inversion method for synthetic aperture radar wind retrieval. J Geophys Res 2002:107, doi:10.1029/2001JC000925.
[48] He Y, Perrie W, Zou Q, et al. A new wind vector algorithm for C-band SAR. IEEE Trans Geosci Remote Sens 2005;43:1453–8.
[49] Song G, Hou Y, Qi P. Wind vector retrieval using dual polarization imagery of ASAR. Prog Nat Sci 2006;16:1183–7.
[50] Thompson DR, Monaldo FM, Winstead NS, et al. Combined estimates improve high-resolution coastal wind mapping. Eos 2001;82:368–74.